Journal of Computational Applied Mechanics 2021, 52(2), 256-270
DOI: 10.22059/jcamech.2021.320044.602

RESEARCH PAPER

# Free vibration analysis of the cracked post-buckled axially functionally graded beam under compressive load

**Emadaldin Sh Khoram-Nejad*, Shapour Moradi, Mohammad Shishehsaz**

Department of Mechanical Engineering, Faculty of Engineering, Shahid Chamran University of Ahvaz, Ahvaz, Iran

**Abstract**
This paper aims to discuss the vibration analysis of the post-buckled cracked axially functionally graded (AFG) beam. The nonlinear equations of motion of the Euler-Bernoulli beam are derived using the equilibrium principles. Then, these differential equations are converted into a set of algebraic ones using the differential quadrature (DQ) method and solved by an arc-length strategy. The resulted displacement field from the post-buckling analysis is assumed to be the equilibrium state of vibration analysis, and an eigenvalue problem is derived. By solving this linear eigenvalue problem, both the natural frequencies and mode shapes of the beam are calculated. The validation of results in comparison with a similar work shows a good agreement. The effect of several parameters such as the extensible and inextensible clamped-clamped boundary conditions, initial geometric imperfection, crack's depth, and crack's location on the natural frequencies and mode shapes are investigated in detail.
**Keywords:** Free Vibration, Axially functionally graded beam, Crack, Differential quadrature method, Initial geometric imperfection, Post-buckling.

## Introduction

Functionally graded (FG) materials are some kinds of materials with various properties along with one or more specific directions. The more common functionally graded structures have variable properties through their thickness [1-6]. Besides, A group of structures made of functionally graded material has variable properties in two or three directions [5, 7-9]. However, when we talk about the beams, it is more helpful that the properties vary along the axial direction. So, the purpose of this paper is to investigate the free vibration of the post-buckled cracked axially functionally graded (AFG) beams under uniaxial compressive load.
The beam is a long and slender structure whose cross-section is small relative to its length. However, if the thickness-to-length ratio increases, shear deformations have significant effects on the beam's behavior. Amara et al. [10] have examined the effect of different shear deformation theories on the post-buckling behavior of FG beams. Emam [11], in his study, has examined the effect of different shear deformation theories on the nonlinear post-buckling of composite beams. The results show that the classical and first-order shear deformation theories (FSDT) predict a smaller amplitude of buckling load than the actual one. This study showed that if the length-to-thickness ratio is more than 50 times, the effects of shear deformation can be ignored. Besides, many researchers ignore the effects of shear deformation and rotary inertia to investigate the behavior of the beams [1, 12-14].
One of the things that have made FG materials superior to other materials is their temperature variable properties. Many types of research have been done on the post-buckling behavior of FG beams due to the thermal load [15-18]. The significant temperature difference at the two

* Corresponding author e-mail: eshkhoramnejad@mscstu.scu.ac.ir

ends of the beam is a more common problem than the temperature difference through the thickness. Therefore, the most appropriate choice is to use AFG beams instead of the conventional FGM beams.

Using variable cross-section areas along the structures' length is of interest in various studies [18-22]. It is also a good idea to use variable properties through the length of structures to reduce the stress concentration caused by changing the cross-sectional area in AFG beams. For the AFG beams, Huang et al. [23] examined the buckling behavior of the AFG beam with a variable cross-section through the length. Shahba and Rajasekaran [24] examined the free vibration and stability of AFG beams in their study. They mentioned that the differential quadrature element method of lowest-order (DQEL) and differential transform element method (DTEM) would be used frequently in the future for modeling the axially functionally graded materials. Huang and Jian [25] have also studied the natural frequencies of the AFG beam.

Other studies have been performed on the post-buckling behavior and vibration of the functionally graded structures. Cai et al. [26] have examined the post-buckling behavior of AFG beams under the distributed transverse and axial loads. The AFG Cantilever beam under a non-follower compressive force has been investigated by Akbas [27]. In this analysis, he considered the three-dimensional model of the beam using an eight-node quadratic element. He solved the nonlinear finite element equations using the displacement control approach in the Newton-Raphson method. In another study, Akbas [28] use finite element analysis to investigate the geometrically nonlinear static of the AFG beams subjected to a point load. Mohammadi and Rastgo [29] study the behavior of FG/lipid nanoplate by considering porosity distribution. The behavior of a porous FG Euler-Bernoulli nanobeam resting on a nonlinear foundation and subjected to mechanical and electrical loads is investigated by Mohammadi et al. [1]. Shariat et al. [30] have worked on the vibration and stability of moving viscoelastic AFG nanobeams aiming at the stability enhancement of translating nano-systems. They show that the non-local effect in their system can be significantly damped by fine-tuning axial material distribution. Also, they conclude that the stability and dynamic responses of axially moving nano-systems enhance using AFG materials instead of homogenous ones. Jin et al. [31] studied the static and dynamic snap-through behaviors of imperfect post-buckled FG-GRC sandwich beams. They also studied the FG-GRC sandwich beam's snap-through behavior by plotting the load-deflection curves and amplitude-frequency bifurcation curves. They concluded that the initial imperfection significantly influences the bending and vibration of the post-buckled beam. These influences are strong only near the critical buckling load of the beam.

The existence of defects in structures has always been of interest to researchers. The presence of a crack in the beams is one of the dangerous defects in these structures and will reduce the local stiffness. Moradi and Jamshidi Moghaddam [13] examined the free vibrations of a post-buckled cracked beam using the differential quadrature method. They have modeled the crack as a rotational and linear spring. Akbas [32] study the post-buckling of a cracked circular column under non-follower axial compression load. The cracked column is modeled as an assembly of two sub-columns connected by a massless elastic rotational spring. Akbas [33] addresses a cracked fiber-reinforced composite (FRC) post-buckling behavior under compressive load in another study. Ke et al. [34] have investigated the post-buckling state of the Timoshenko cracked FG beam under end shortening. They found that the intact and cracked beam's post-buckling state's deflection behavior and configuration are similar. Akbas [27] has studied the effect of the depth and location of cracks on the behavior of its post-buckled configuration. He also showed that using an FG material for beams can reduce the local stiffness caused by the crack's presence.

The effect of crack on the free vibration of a post-buckled AFG beam has not been seriously investigated. Also, there are two scenarios to investigate the vibration of the buckled beams if the boundary condition is movable along the compressive load direction. To the author's best knowledge, less attention to these issues is pending. Therefore, the purpose of the current study is to investigate the free vibration of a clamped-clamped buckled cracked AFG Euler-Bernoulli beam under a compressive load in two boundary conditions for vibration of the buckled beam.

## Theory and modelling

As can be seen from Figure 1, to obtain the beam equations, a beam with length $l$, thickness $h$, and width b made of axially functionally graded material has been considered. The coordinate's origin of the problem is located at the $x = 0$, and an open-edge crack with depth $a$ located at $x = l_c$.

This study is made up of two-phase analysis. The first analysis is a nonlinear post-buckling analysis of the beam under axially compressive load acted at $x = l$ to find the static post-buckled state. The second analysis is a vibration analysis about the post-buckled state. By solving the first analysis using the arc-length method, a displacement field is obtained that is considered as the post-buckled state for the second analysis. In the vibration analysis, equations of motion are linearized, and the resulted eigenvalue problem is figured out to turn over the frequencies and mode shapes.

The boundary conditions of the beam in this study are clamped-clamped. Consider Figure 1, where the right end boundary condition must be movable along the $x$-axis to apply an axial load at $x = l$. After the post-buckling analysis is done, two kinds of boundary conditions will be possible for vibration analysis. First, the right end boundary condition will remain the same as the post-buckling analysis, and no change will happen (case 1 in Figure 1). In the second case, the beam's right end boundary condition will have no displacement in the x-direction. The first and second cases are called the inextensible and extensible models of the clamped-clamped boundary conditions, respectively. The importance of these kinds of boundary conditions is clearly shown in the following sections.

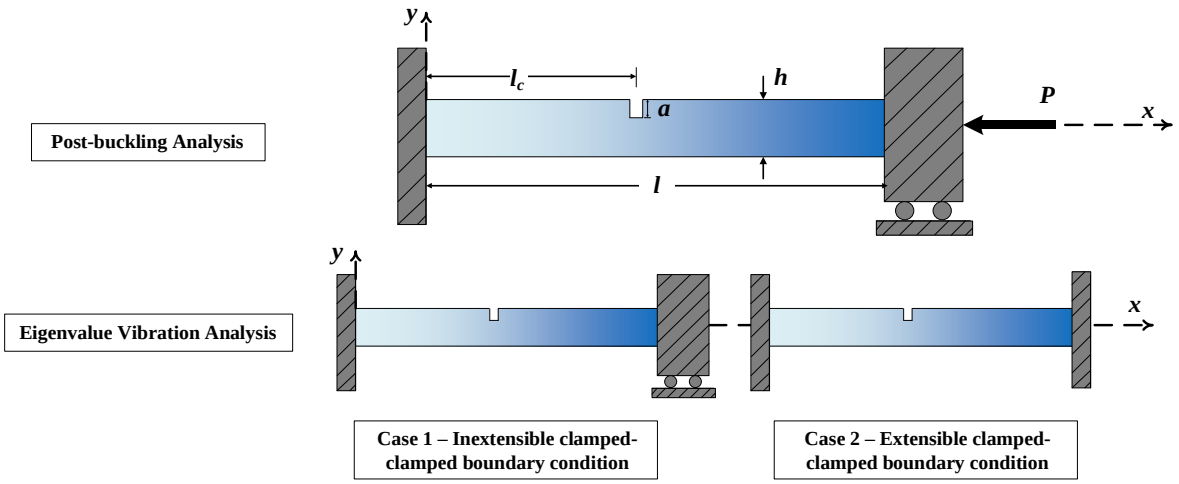


**Figure 1.** All of the boundary conditions studying in this paper

*Distribution of material properties in axially functionally graded (AFG) beam*

The distribution of material properties in this study varies along the beam's length following the simple power-law distribution shown in Equation 1. So, the right side of this beam ($x = l$)

is completely made of metal, and the left side ($x = 0$) is made of pure ceramic. In this study, the passion ratio remains 0.3 as a constant value. The ceramic and metal are considered as Silicon-Nitride (with $E_c$ = 348.43 GPa and $\rho_c$ = 2370 Kg / m$^3$) and Stainless Steel with ($E_m$ = 201.04 GPa and $\rho_c$ = 8166 Kg / m$^3$), respectively.

$$\bar{P}(x) = (\bar{P}_L - \bar{P}_R)\left[1 - \left(\frac{x}{l}\right)^k\right] + \bar{P}_R \tag{1}$$

where $\bar{P}$ represents the material's variable property along the length of the beam, subscripts $L$ and $R$ also indicate its value on the left ($x = 0$) and right ($x = l$) ends of the beam, respectively. Figure 2 shows the changes in Young's modulus in the AFG beam along its length. The equivalent Young's modulus and density of the axially functionally graded beam are calculated as:

$$E_{AFG} = \frac{E_c + kE_m}{1+k}, \quad \rho_{AFG} = \frac{\rho_c + k\rho_m}{1+k} \tag{2}$$

Also, the critical buckling load is calculated as Equation 3:

$$P_{cr} = \frac{\pi^2 E_{AFG} I}{l_{eff}^2} \tag{3}$$

where $l_{eff}$ is the effective length of the beam, and as it is evident for clamped-clamped beams, it is chosen as one-fourth of the beam's actual length.

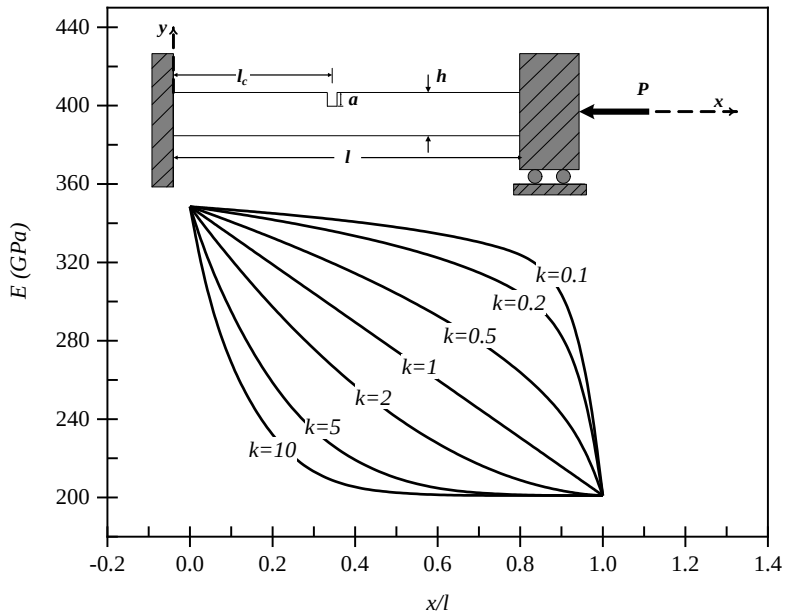


**Figure 2.** Distribution of the Young's modulus of the AFG beam along with its length

*Crack modelling*

To model the cracked AFG beam, one may assume that the crack never grows. Therefore it can be modeled using a linear and rotational spring. This assumption is reasonably valid if the problem is studied from a macroscopic view. Therefore, the cracked beam is modeled as two beams connected with the linear and rotational spring. The presence of cracks induces local compliance in the beam, and different expressions have been proposed to evaluate the compliance coefficients of the crack depending on the load applied to the beam [35]. In this study, an axial compressive load was applied and acted upon the center of the beam's cross-section. Using the Paris equation, Castigliano's theory, the assumption of linear elastic

fracture mechanics (LEFM), and the plane-stress problem, the crack compliance coefficient, c, can be obtained as following [13]:

$$c = \frac{72\pi}{E\ x\ h^2 b}\int_0^{\bar{a}} \bar{\alpha} F^2\ \bar{\alpha}\ d\bar{\alpha}, \quad \bar{a} = a/h, \quad \bar{\alpha} = \alpha/h \tag{4}$$

where $E$ is Young's modulus of the beam, which varies along with its length and is calculated by Equation 1, the correction function of the stress intensity factor, $F$, depends on the differences in geometry and applied loads [34], and may be defined as follows:

$$F(\bar{\alpha}) = \sqrt{\frac{\tan\lambda}{\lambda}}\left[0.923 + 0.199(1-\sin\lambda)^4\right] \Big/ \cos\lambda, \quad \lambda = \frac{\pi\bar{\alpha}}{2} \tag{5}$$

*Equations of motion*

The nonlinear differential equations of motion for a post-buckled cracked beam are extracted as follow [13]:

$$\begin{aligned}
&w_{,x} - \left(1 + \frac{N}{K_{ext}}\right)\sin\theta + \sin\theta_0 = 0,\\
&u_{,x} - \left(1 + \frac{N}{K_{ext}}\right)\cos\theta + \cos\theta_0 = 0,\\
&K_{ben}\left[\theta_{,x} - \theta_{0,x}\right] - M = 0,\\
&M_{,x} + Q = 0,\\
&N\sin\theta_{,x} + Q\cos\theta_{,x} = \rho A\ddot{w},\\
&N\cos\theta_{,x} - Q\sin\theta_{,x} = \rho A\ddot{u}
\end{aligned} \tag{6}$$

where $N$, $Q$, and $M$ are the axial force, shear force, and bending moment, respectively. Also, $w$, $u$, and $\theta$ are displacements of the beam's neutral axis in the y and x directions and the beam's rotation around the $z$-axis, respectively. $K_{ben} = EI$ shows the bending stiffness, and the stretching stiffness is defined as $K_{ext} = EA$. $A$ is the cross-section area, and ρ is the equivalent density of the AFG beam, calculated from Equation 2.

These equations are obtained by considering the equilibrium principles for a small differential element of the beam with an initial geometric imperfection. It is assumed that the effects of rotary inertia and shear deformation are negligible (Euler-Bernoulli beam theory). This imperfection appears as the initial angle, $\theta_0$, in the equations. For clamped-clamped beams, the imperfection can be presented by the following equation:

$$\bar{W} = \frac{1}{2}W_0\ 1 - \cos\ 2\pi x \tag{7}$$

where, $W_0$ is the amplitude of the initial imperfection and is assumed to be 0.001 m throughout this study.

Using the fact that the vibration displacement field oscillates around its equilibrium state, the total displacement field of the AFG beam is introduced as Equation 8.

$$
\begin{aligned}
w &= w_s + w_d e^{-i\omega t},\\
u &= u_s + u_d e^{-i\omega t},\\
\theta &= \theta_s + \theta_d e^{-i\omega t},\\
Q &= Q_s + Q_d e^{-i\omega t},\\
N &= N_s + N_d e^{-i\omega t},\\
M &= M_s + M_d e^{-i\omega t}
\end{aligned}
\tag{8}
$$

where *s*, *d*, $\omega$, and *t*, indicate the static equilibrium state of the AFG beam, dynamic oscillation about the static equilibrium, natural frequency, and time, respectively. By substituting Equation 8 into Equation 6 and neglecting the dynamic part of the displacement field and the time-dependent terms, the static nonlinear differential equations of the AFG beam are derived as follow:

$$
\begin{aligned}
&w_{s,x} - \left(1 + \frac{N_s}{K_{ext}}\right)\sin\theta_s + \sin\theta_0 = 0,\\
&u_{s,x} - \left(1 + \frac{N_s}{K_{ext}}\right)\cos\theta_s + \cos\theta_0 = 0,\\
&K_{ben}\left[\theta_{s,x} - \theta_{0,x}\right] - M_s = 0,\\
&M_{s,x} + Q_s = 0,\\
&N_s \sin\theta_{s\ ,x} + Q_s \cos\theta_{s\ ,x} = 0,\\
&N_s \cos\theta_{s\ ,x} - Q_s \sin\theta_{s\ ,x} = 0
\end{aligned}
\tag{9}
$$

Such a nonlinear set of coupled differential equations may be difficult or even impossible to solve. Therefore, many approaches have been suggested to simplify this problem by converting them into algebraic ones. One of these methods is the differential quadrature method (DQM). In this method, the derivative of a function with respect to one of its variables is calculated by the weighting sum of the functions at some intermediate points. Using the Gauss-Lobatto-Chebyshev sample points, the nonlinear static differential equations (Equation 9) are converted to a set of the nonlinear algebraic equation by the following equations:

$$
\begin{aligned}
&\sum_{j=1}^{n_p} C_{ij} w_{sj} - \left(1 + \frac{N_{si}}{K_{ext}}\right)\sin\theta_{si} + \sin\theta_{0i} = 0,\\
&\sum_{j=1}^{n_p} C_{ij} u_{sj} - \left(1 + \frac{N_{si}}{K_{ext}}\right)\cos\theta_{si} + \cos\theta_{0i} = 0,\\
&\sum_{j=1}^{n_p} C_{ij}\theta_{sj} - \theta_{0i,x} - \frac{M_{si}}{K_{ben}} = 0,\\
&\sum_{j=1}^{n_p} C_{ij} M_{sj} - Q_{si} = 0,\\
&\left(\sum_{j=1}^{n_p} C_{ij} N_{sj}\right)\sin\theta_{sj} + \left(\sum_{j=1}^{n_p} C_{ij}\theta_{sj}\right) N_{sj}\cos\theta_{sj} + \left(\sum_{j=1}^{n_p} C_{ij} Q_{sj}\right)\cos\theta_{sj} - \left(\sum_{j=1}^{n_p} C_{ij}\theta_{sj}\right) Q_{sj}\sin\theta_{sj} = 0,\\
&\left(\sum_{j=1}^{n_p} C_{ij} N_{sj}\right)\cos\theta_{sj} - \left(\sum_{j=1}^{n_p} C_{ij}\theta_{sj}\right) N_{sj}\sin\theta_{sj} - \left(\sum_{j=1}^{n_p} C_{ij} Q_{sj}\right)\sin\theta_{sj} - \left(\sum_{j=1}^{n_p} C_{ij}\theta_{sj}\right) Q_{sj}\cos\theta_{sj} = 0,
\end{aligned}
\tag{10}
$$

This set of nonlinear equations can be solved by an arc-length strategy to set the equilibrium state for vibration analysis. Then by substituting Equation 8 into Equation 6 and neglecting the static and nonlinear terms (small-amplitude vibration), the pre-stress linearized free vibration differential equations are obtained as Equation 11.

$$
\begin{aligned}
&w_{d,x}-\left(1+\frac{N_s}{K_{ext}}\right)\theta_d\cos\theta_s-\frac{N_d}{K_{ext}}\sin\theta_s=0\\
&u_{d,x}+\left(1+\frac{N_s}{K_{ext}}\right)\theta_d\sin\theta_s-\frac{N_d}{K_{ext}}\cos\theta_s\\
&\theta_{d,x}-\frac{M_d}{K_{ben}}=0\\
&M_{d,x}-Q_d=0\\
&N_d\sin\theta_s+N_s\theta_d\cos\theta_s{}_{,x}+Q_d\cos\theta_s-Q_s\theta_d\sin\theta_s{}_{,x}=-\omega^2\rho Aw_d\\
&N_d\cos\theta_s-N_s\theta_d\sin\theta_s{}_{,x}-Q_d\sin\theta_s+Q_s\theta_d\cos\theta_s{}_{,x}=-\omega^2\rho Au_d
\end{aligned}
\tag{11}
$$

Similar to the static analysis, Equation 11 converted to a set of the algebraic equation using the DQ method as follow:

$$
\begin{aligned}
&\sum_{j=1}^{n_p}C_{ij}w_{dj}-\left(1+\frac{N_{si}}{K_{ext}}\right)\theta_{di}\cos\theta_{si}-\frac{N_{di}}{K_{ext}}\sin\theta_{si}=0,\\
&\sum_{j=1}^{n_p}C_{ij}u_{dj}+\left(1+\frac{N_{si}}{K_{ext}}\right)\theta_{di}\sin\theta_{si}-\frac{N_{di}}{K_{ext}}\cos\theta_{si}=0,\\
&\sum_{j=1}^{n_p}C_{ij}\theta_{dj}-\frac{M_{di}}{K_{ben}}=0,\\
&\sum_{j=1}^{n_p}C_{ij}M_{dj}-Q_{di}=0,\\
&\sum_{j=1}^{n_p}C_{ij}\left(N_{dj}\sin\theta_{sj}+N_{sj}\theta_{dj}\cos\theta_{sj}\right)+\sum_{j=1}^{n_p}C_{ij}\left(Q_{dj}\cos\theta_{sj}-Q_{sj}\theta_{dj}\sin\theta_{sj}\right)=-\omega^2\rho Aw_{di},\\
&\sum_{j=1}^{n_p}C_{ij}\left(N_{dj}\cos\theta_{sj}-N_{sj}\theta_{dj}\sin\theta_{sj}\right)+\sum_{j=1}^{n_p}C_{ij}\left(Q_{dj}\sin\theta_{sj}+Q_{sj}\theta_{dj}\cos\theta_{sj}\right)=-\omega^2\rho Au_{di},
\end{aligned}
\tag{12}
$$

*Boundary and continuity conditions*

The continuity and discontinuity conditions where the two beam elements are connected for the post-buckling analysis are defined as follow:

$$
\begin{aligned}
&u_s^1\ l_c=u_s^2\ l_c\ ,\quad w_s^1\ l_c=w_s^2\ l_c\ ,\quad M_s^1\ l_c=M_s^2\ l_c\ ,\\
&F_{sx}^1\ l_c=F_{sx}^2\ l_c\ ,\quad F_{sy}^1\ l_c=F_{sy}^2\ l_c\ ,\quad \theta_s^1\ l_c=\theta_s^2\ l_c-cM_s^1\ l_c
\end{aligned}
\tag{13}
$$

where

$$
F_{sx}=N_s\cos\theta_s-Q_s\sin\theta_s\,,\quad F_{sy}=N_s\sin\theta_s+Q_s\cos\theta_s \tag{14}
$$

Similar conditions are defined for the vibration analysis as:

$$
\begin{aligned}
&u_d^1\ l_c=u_d^2\ l_c\ ,\quad w_d^1\ l_c=w_d^2\ l_c\ ,\quad M_d^1\ l_c=M_d^2\ l_c\ ,\\
&F_{dx}^1\ l_c=F_{dx}^2\ l_c\ ,\quad F_{dy}^1\ l_c=F_{dy}^2\ l_c\ ,\quad \theta_d^1\ l_c=\theta_d^2\ l_c-cM_d^1\ l_c
\end{aligned}
\tag{15}
$$

where

$$F_{dx} = N_d \cos\theta_s - N_s\theta_d \sin\theta_s - Q_d \sin\theta_s - Q_s\theta_d \cos\theta_s,$$
$$F_{sy} = N_d \sin\theta_s + N_s\theta_d \cos\theta_s + Q_d \cos\theta_s - Q_s\theta_d \sin\theta_s \quad (16)$$

The clamped-clamped boundary conditions for the post-buckling analysis are defined as:

$$u_s^1\ 0\ = 0, \quad w_s^1\ 0\ = 0, \quad \theta_s^1\ 0\ = 0,$$
$$N_s^2(l) = P, \quad w_s^2\ l\ = 0, \quad \theta_s^2\ l\ = 0 \quad (17)$$

The clamped-clamped boundary condition for vibration analysis is defined in extensible and inextensible forms. For extensible form:

$$u_d^1\ 0\ = 0, \quad w_d^1\ 0\ = 0, \quad \theta_d^1\ 0\ = 0,$$
$$u_d^2\ l\ = 0, \quad w_d^2\ l\ = 0, \quad \theta_d^2\ l\ = 0 \quad (18)$$

and for inextensible form:

$$u_d^1\ 0\ = 0, \quad w_d^1\ 0\ = 0, \quad \theta_d^1\ 0\ = 0,$$
$$N_d^2\ l\ = 0, \quad w_d^2\ l\ = 0, \quad \theta_d^2\ l\ = 0 \quad (19)$$

Equation 12 is a non-standard eigenvalue problem. By converting it to a standard eigenvalue problem, the natural frequencies and mode shapes can be evaluated.

## Results

In this section, the natural frequencies and mode shapes of cracked buckled axially functionally graded beams under uniaxial compressive load are investigated. A crack with a relative depth of 0.4 is located at the middle of the beam. The length, width, and height of this AFG beam are 1000 mm, 25 mm, and 10 mm, respectively. For avoiding the bifurcation-type buckling, it is assumed that the beam has an initial geometric imperfection with the amplitude of 0.001 m in the form of the first buckling mode shape.

Two sub-beams are assumed to be connected by a linear and rotational spring at the crack location to model this beam. A convergence test is performed to check the accuracy of the DQ method. Figure 3 shows the first non-dimensional natural frequency of the beam mentioned above for a different number of sampling points. As shown by the figure, the natural frequency converges quickly, and the number of sampling points is chosen to be eleven in each sub-beam.

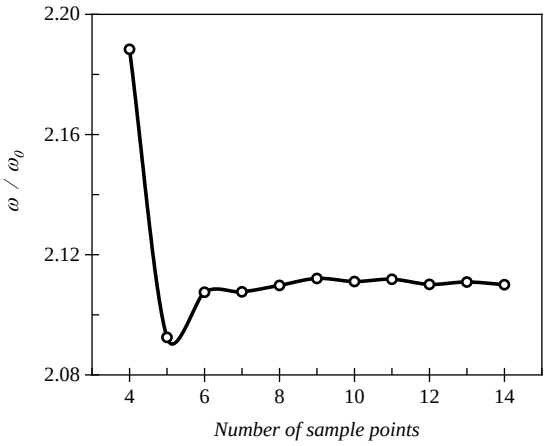


**Figure 3.** Convergence of the sample points in differential quadrature method for each beam's element ($\omega_0 = \frac{1}{l^2}\sqrt{E_{AFG} I / \rho_{AFG} A}$)

As shown in Table 1, the presented formulations' validation is checked with the first four non-dimensional natural frequencies mentioned in the published literature [13]. There is a good agreement between the results. The maximum relative error is less than 1.3 percent of the fourth natural frequency of the relative load 1.4.
In this table, $P$ is the axial compressive load acted upon the right end of the beam (Figure 1), and $P_{cr}$ is the critical load of the intact beam that can be calculated from Equation 3.

**Table 1.** Comparison of the first four non-dimensional natural frequencies of the beam

| Relative load ($P/P_{cr}$) | Nat. Freq. | DQM- Presented | Ref. [13] | Relative error (%) |
|---|---|---|---|---|
| 1.2 | $\omega_1/\omega_0$ | 12.5250 | 12.5447 | 0.157 |
| | $\omega_2/\omega_0$ | 6.5264 | 6.5964 | 1.061 |
| | $\omega_3/\omega_0$ | 30.9111 | 30.7925 | 0.385 |
| | $\omega_4/\omega_0$ | 17.4578 | 17.6030 | 0.825 |
| 1.4 | $\omega_1/\omega_0$ | 13.1548 | 13.2634 | 0.819 |
| | $\omega_2/\omega_0$ | 5.5601 | 5.6031 | 0.767 |
| | $\omega_3/\omega_0$ | 26.3558 | 26.4738 | 0.446 |
| | $\omega_4/\omega_0$ | 14.5140 | 14.6918 | 1.210 |

The effect of the axial compressive load on the first four non-dimensional natural frequencies for both the extensible and inextensible clamped-clamped AFG beams is shown in Figure 4. The frequencies are smoothly dropped in the pre-buckling state (from load *0* to about 0.8*Pcr*) for both boundary conditions. However, there are fundamental differences in the frequency behavior of these two kinds of boundary conditions in the post-buckling state. For the relative load of about *0.8* to *1.0* in the inextensible case, the first frequency is becoming unstable and then recovered and became stable again. There is no interaction between mode shapes of the beam with inextensible boundary conditions. After buckling occurs, the first frequency increases abruptly for the extensible boundary condition and makes interactions with the second, third and fourth mode shapes.

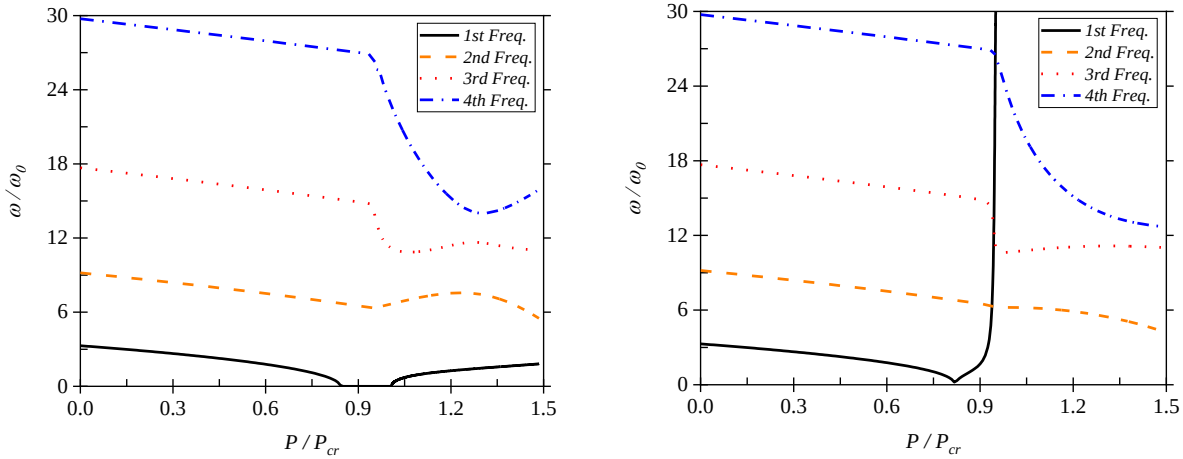


**Figure 4.** Variation of the real part of non-dimensional frequencies of the AFG beam with respect to axial load with a) inextensible and b) extensible clamped-clamped boundary conditions.

In Figure 5, the mode shapes for extensible boundary condition under two different axial loads is shown. For the relative load of *0.5*, the first mode shape has no node, and the second, third, and fourth ones have one, two, and three nodes, respectively. At the post-buckling state for the relative load of *1.10*, the first, second, third, and fourth shape modes have one, two, three, and four nodes. Figure 4 and Figure 5 conclude that the first mode has a completely different behavior compared with others. This behavior is due to the boundary conditions in

the axial direction. Such modes are called the extensional modes and are affected by the bending stiffness and the stretching-induced stiffness.
On the contrary, other modes are called the bending modes and are only affected by the bending stiffness. When the AFG beam is under axial compressive load, due to an increase in the beam's load and curvature, the bending stiffness is reduced. Therefore, the natural frequencies of the bending modes are decreased, as shown in Figure 4, and the extensional modes are increased.

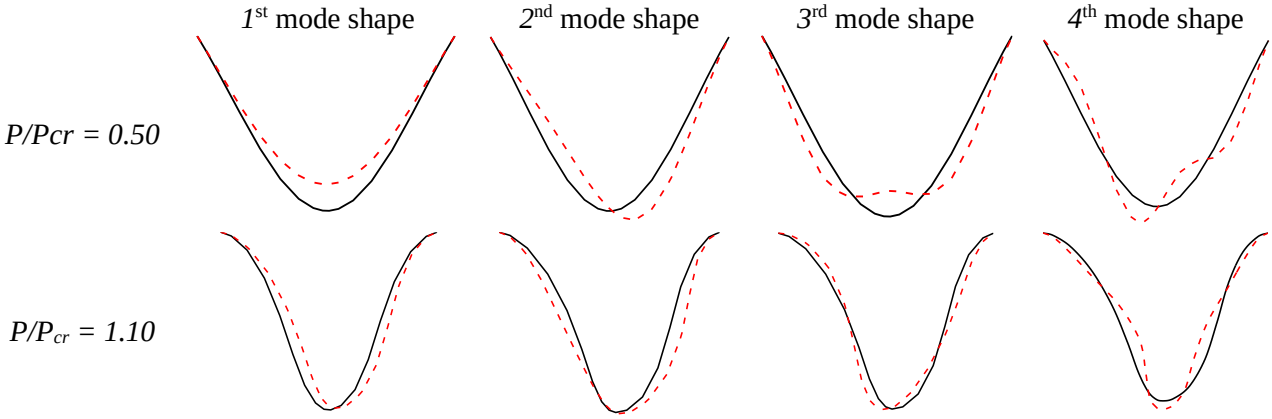


**Figure 5.** Mode shapes of the AFG beam with extensible boundary condition

Besides, the behavior of the mode shapes of the inextensible clamped-clamped AFG beam about its post-buckling state is investigated in Figure 6. As shown from this figure, both the first and second modes' behavior is like stretching modes and different from others (especially at the right end of the beam). Thus, one can conclude that the first and second mode shapes are stretching modes and others are bending ones.

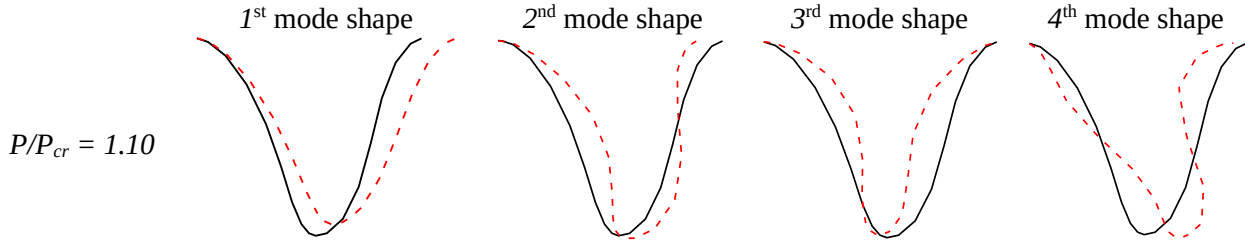


**Figure 6.** Mode shapes of the AFG beam with inextensible boundary condition

The effect of the various initial geometric imperfection on the instability and re-stabilization behavior of the first natural frequency in Figure 4 is investigated. As shown in Figure 7, by increasing the amplitude of the initial imperfection from 0.001 m to 0.1 m, the first frequency becomes stable in all of its ranges.
The variation of the crack's depth on the first four non-dimensional natural frequencies is investigated for both pre-and post-buckling states in Figure 8. In the pre-buckling state (relative load 0.5), all of the frequencies are decreased by increasing the crack's depth due to reduced bending stiffness. In this state, stretching-induced stiffness is not increased with decreased bending stiffness, so the total stiffness is reduced for the first mode.

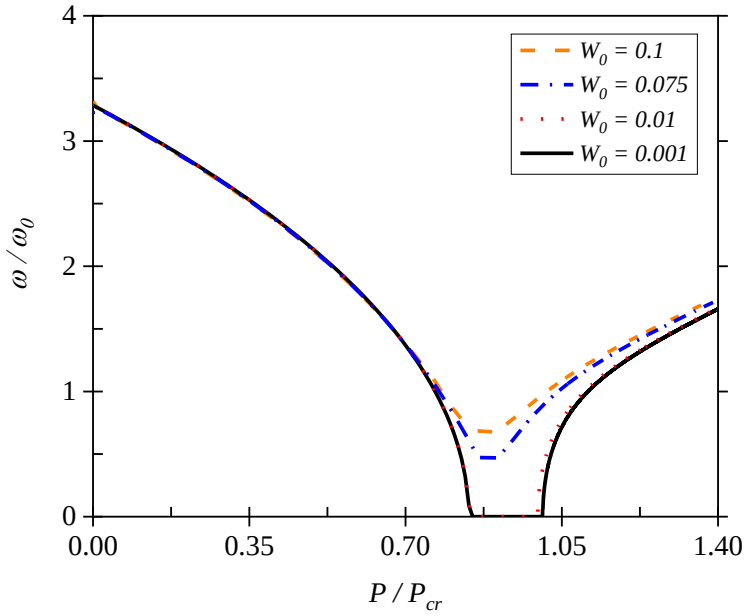


**Figure 7.** Effect of initial imperfection on the stability of first frequency for inextensible clamped boundary conditions

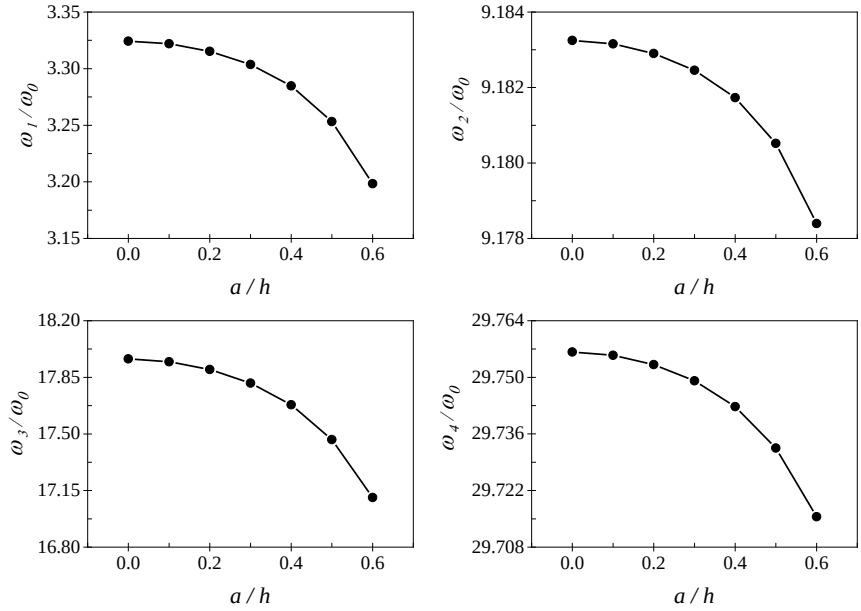


**Figure 8.** Effect of crack's depth on the frequencies of the unloaded AFG beam with extensible clamped boundary condition (for $l_c / l = 0.5$)

For a post-buckled beam (relative load 1.2), the increase in the stretching-induced stiffness dominates the decreasing of the bending stiffness. As shown in Figure 9, the first and second frequencies are increased with the increase of the crack's depth (because they are stretching modes), and other frequencies decreased.

Figure 10 reveals the effect of crack's location with relative depth 0.4 and 0.6 on the first four non-dimensional natural frequencies. It can be seen that at the specified crack's location, the frequencies are approximately constant for both crack depths. These are the locations of the mode shape's nodes. The number of nodes that can be calculated from this figure is the same as those of the node's number in the pre-buckling state (Figure 5). Also, it can be concluded from Figure 10 that when the crack is in the dominant ceramic regions, the frequencies are reduced.

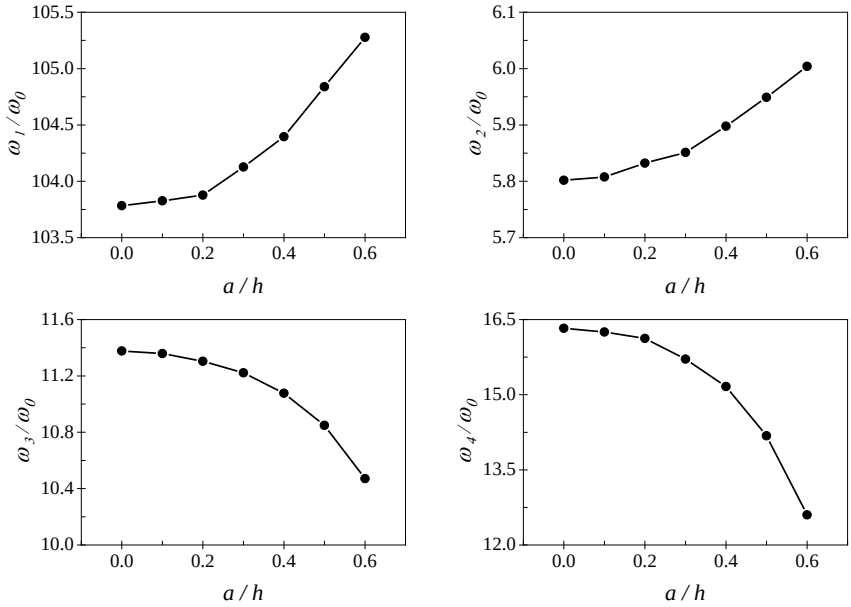


**Figure 9.** Effect of crack's depth on the frequencies of the post-buckled AFG beam with extensible clamped boundary condition (for $l_c/l = 0.5$)

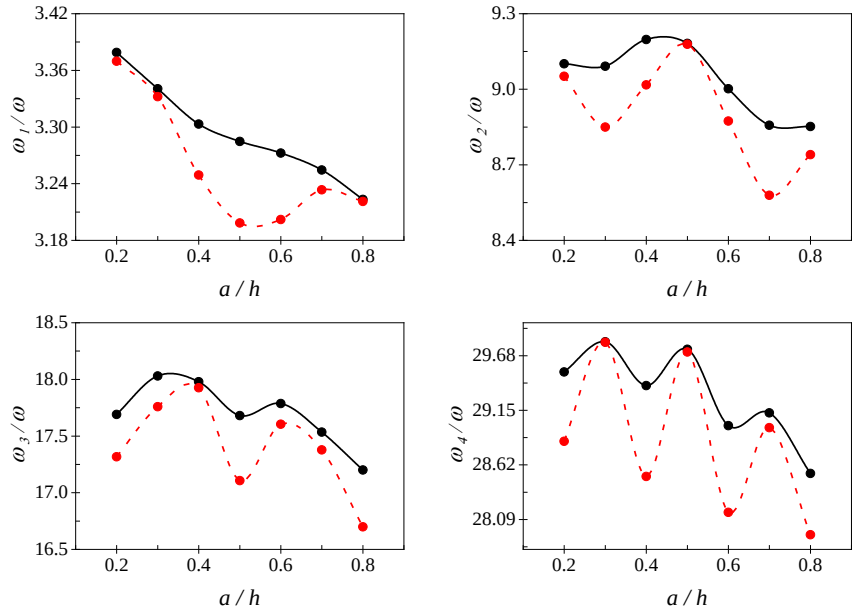


**Figure 10.** Effect of crack's location on the natural frequencies of the un-loaded AFG beam (- crack depth 0.4 and -- crack depth 0.6)

## Conclusion

The vibration of the buckled cracked axially functionally graded beam is investigated in this paper. Very few publications can be found that address the difference between the extensible and inextensible clamped-clamped boundary conditions of an AFG beam. A crack divides the beam into two sub-beams using a linear and rotational spring model. It is assumed that the beam is a slender beam that the shear deformation and rotary inertia effects are negligible (Euler-Bernoulli beam theory). The equilibrium principles are used to derive the beam's nonlinear governing equations. These equations are converted into algebraic ones using the differential quadrature method (DQM) and solved by an arc-length strategy. The free

vibration took place around the post-buckled equilibrium state. By solving the linear eigenvalue problem, both the natural frequencies and mode shapes of the beam were computed. The accuracy of the results compared with those of the published literature and several parameters affecting the natural frequencies of the AFG beam are investigated.

The results showed a big difference between the natural frequencies and mode shapes of the extensible and inextensible clamped-clamped boundary conditions. Using these differences to obtain the AFG beam's mode shapes' behavior is an essential result of this paper. The stretching-induced stiffness depends on the boundary conditions and loads in the x-direction. The stretching mode shapes are detected by investigating the beams with extensible boundary conditions.

For the beam with extensible boundary conditions, increasing the crack's depth, the bending and stretching modes' frequency are decreased and increased, respectively. Besides, there are some displacements along the x-direction at the right boundary conditions in the stretching modes. At the same time, there is no displacement in the x-direction in the bending modes.

The initial geometric imperfection was used in this study to avoid the bifurcation-type buckling. It was shown that the frequency near the critical load is becoming more stable and increased by increasing the initial imperfection amplitude. The initial imperfection effect on the frequencies is strong only near the critical load and can be neglected as the load increases. When the applying load increases, the ratio between the initial imperfection and the AFG beam's deflection tends to zero.

The crack properties were a part of this study. It can be concluded that by increasing the crack's depth, the natural frequencies are reduced due to the reduction in bending stiffness. However, for a post-buckled AFG beam, the increase in stretching-induced stiffness overcomes the reduction of bending stiffness in the stretching modes. As a consequence, the frequencies of the stretching mode are increased by increasing the crack's depth. Crack's location is another parameter that was investigated. From the results, it can be concluded that if the crack is located on the nodes of a vibrational mode shape, the frequencies will approximately remain constant by changing the crack's depth.

## References

[1] M. Mohammadi, M. Hosseini, M. Shishesaz, A. Hadi, A. Rastgoo, Primary and secondary resonance analysis of porous functionally graded nanobeam resting on a nonlinear foundation subjected to mechanical and electrical loads, *European Journal of Mechanics-A/Solids,* Vol. 77, pp. 103793, 2019.

[2] M. Shishesaz, M. Hosseini, Mechanical behavior of functionally graded nano-cylinders under radial pressure based on strain gradient theory, *Journal of Mechanics,* Vol. 35, No. 4, pp. 441-454, 2019.

[3] A. Daneshmehr, A. Rajabpoor, A. Hadi, Size dependent free vibration analysis of nanoplates made of functionally graded materials based on nonlocal elasticity theory with high order theories, *International Journal of Engineering Science,* Vol. 95, pp. 23-35, 2015.

[4] M. Zamani Nejad, M. Jabbari, A. Hadi, A review of functionally graded thick cylindrical and conical shells, *Journal of Computational Applied Mechanics,* Vol. 48, No. 2, pp. 357-370, 2017.

[5] M. Gharibi, M. Zamani Nejad, A. Hadi, Elastic analysis of functionally graded rotating thick cylindrical pressure vessels with exponentially-varying properties using power series method of Frobenius, *Journal of Computational Applied Mechanics,* Vol. 48, No. 1, pp. 89-98, 2017.

[6] Z. Mazarei, M. Z. Nejad, A. Hadi, Thermo-elasto-plastic analysis of thick-walled spherical pressure vessels made of functionally graded materials, *International Journal of Applied Mechanics,* Vol. 8, No. 04, pp. 1650054, 2016.
[7] A. Barati, A. Hadi, M. Z. Nejad, R. Noroozi, On vibration of bi-directional functionally graded nanobeams under magnetic field, *Mechanics Based Design of Structures and Machines*, pp. 1-18, 2020.
[8] M. Z. Nejad, A. Hadi, A. Rastgoo, Buckling analysis of arbitrary two-directional functionally graded Euler–Bernoulli nano-beams based on nonlocal elasticity theory, *International Journal of Engineering Science,* Vol. 103, pp. 1-10, 2016.
[9] A. Hadi, M. Z. Nejad, M. Hosseini, Vibrations of three-dimensionally graded nanobeams, *International Journal of Engineering Science,* Vol. 128, pp. 12-23, 2018.
[10] K. Amara, M. Bouazza, B. Fouad, Postbuckling analysis of functionally graded beams using nonlinear model, *Periodica Polytechnica Mechanical Engineering,* Vol. 60, No. 2, pp. 121-128, 2016.
[11] S. A. Emam, Analysis of shear-deformable composite beams in postbuckling, *Composite structures,* Vol. 94, No. 1, pp. 24-30, 2011.
[12] M. Mohammadi, M. Safarabadi, A. Rastgoo, A. Farajpour, Hygro-mechanical vibration analysis of a rotating viscoelastic nanobeam embedded in a visco-Pasternak elastic medium and in a nonlinear thermal environment, *Acta Mechanica,* Vol. 227, No. 8, pp. 2207-2232, 2016.
[13] S. Moradi, P. J. Moghadam, Vibration analysis of cracked post-buckled beams, *Applied Mathematical Modelling,* Vol. 38, No. 13, pp. 3281-3294, 2014.
[14] M. Baghani, M. Mohammadi, A. Farajpour, Dynamic and stability analysis of the rotating nanobeam in a nonuniform magnetic field considering the surface energy, *International Journal of Applied Mechanics,* Vol. 8, No. 04, pp. 1650048, 2016.
[15] J.-S. Park, J.-H. Kim, Thermal postbuckling and vibration analyses of functionally graded plates, *Journal of Sound and Vibration,* Vol. 289, No. 1-2, pp. 77-93, 2006.
[16] Y. Kiani, M. R. Eslami, Thermomechanical buckling oftemperature-dependent FGM beams, *Latin American Journal of Solids and Structures,* Vol. 10, No. 2, pp. 223-246, 2013.
[17] S. S. Mirjavadi, S. Rabby, N. Shafiei, B. M. Afshari, M. Kazemi, On size-dependent free vibration and thermal buckling of axially functionally graded nanobeams in thermal environment, *Applied Physics A,* Vol. 123, No. 5, pp. 315, 2017/04/06, 2017.
[18] N. Shafiei, S. S. Mirjavadi, B. M. Afshari, S. Rabby, A. Hamouda, Nonlinear thermal buckling of axially functionally graded micro and nanobeams, *Composite Structures,* Vol. 168, pp. 428-439, 2017.
[19] M. Danesh, A. Farajpour, M. Mohammadi, Axial vibration analysis of a tapered nanorod based on nonlocal elasticity theory and differential quadrature method, *Mechanics Research Communications,* Vol. 39, No. 1, pp. 23-27, 2012.
[20] A. Farajpour, M. Danesh, M. Mohammadi, Buckling analysis of variable thickness nanoplates using nonlocal continuum mechanics, *Physica E: Low-dimensional Systems and Nanostructures,* Vol. 44, No. 3, pp. 719-727, 2011.
[21] N. Shafiei, M. Kazemi, Buckling analysis on the bi-dimensional functionally graded porous tapered nano-/micro-scale beams, *Aerospace Science and Technology,* Vol. 66, pp. 1-11, 2017.

[22] S. Rajasekaran, H. B. Khaniki, Bending, buckling and vibration of small-scale tapered beams, *International Journal of Engineering Science,* Vol. 120, pp. 172-188, 2017.
[23] Y. Huang, M. Zhang, H. Rong, Buckling analysis of axially functionally graded and non-uniform beams based on Timoshenko theory, *Acta Mechanica Solida Sinica,* Vol. 29, No. 2, pp. 200-207, 2016.
[24] A. Shahba, S. Rajasekaran, Free vibration and stability of tapered Euler–Bernoulli beams made of axially functionally graded materials, *Applied Mathematical Modelling,* Vol. 36, No. 7, pp. 3094-3111, 2012.
[25] Y. Huang, X.-F. Li, A new approach for free vibration of axially functionally graded beams with non-uniform cross-section, *Journal of sound and vibration,* Vol. 329, No. 11, pp. 2291-2303, 2010.
[26] K. Cai, D. Y. Gao, Q. H. Qin, Postbuckling analysis of a nonlinear beam with axial functionally graded material, *Journal of Engineering Mathematics,* Vol. 88, No. 1, pp. 121-136, 2014.
[27] Ş. D. Akbaş, Post-buckling analysis of axially functionally graded three-dimensional beams, *International Journal of Applied Mechanics,* Vol. 7, No. 03, pp. 1550047, 2015.
[28] Ş. D. Akbaş, Geometrically nonlinear analysis of axially functionally graded beams by using finite element method, *Journal of Computational Applied Mechanics,* Vol. 51, No. 2, pp. 411-416, 2020.
[29] M. Mohammadi, A. Rastgoo, Primary and secondary resonance analysis of FG/lipid nanoplate with considering porosity distribution based on a nonlinear elastic medium, *Mechanics of Advanced Materials and Structures,* Vol. 27, No. 20, pp. 1709-1730, 2020/10/15, 2020.
[30] A. Shariati, H. Mohammad-Sedighi, K. K. Żur, M. Habibi, M. Safa, On the vibrations and stability of moving viscoelastic axially functionally graded nanobeams, *Materials,* Vol. 13, No. 7, pp. 1707, 2020.
[31] Q. Jin, X. Hu, Y. Ren, H. Jiang, On static and dynamic snap-throughs of the imperfect post-buckled FG-GRC sandwich beams, *Journal of Sound and Vibration,* Vol. 489, pp. 115684, 2020.
[32] Ş. D. Akbaş, Post-buckling analysis of edge cracked columns under axial compression loads, *International Journal of Applied Mechanics,* Vol. 8, No. 08, pp. 1650086, 2016.
[33] Ş. D. Akbaş, Post-buckling analysis of a fiber reinforced composite beam with crack, *Engineering Fracture Mechanics,* Vol. 212, pp. 70-80, 2019.
[34] L.-L. Ke, J. Yang, S. Kitipornchai, Postbuckling analysis of edge cracked functionally graded Timoshenko beams under end shortening, *Composite Structures,* Vol. 90, No. 2, pp. 152-160, 2009.
[35] C. Karaagac, H. Öztürk, M. Sabuncu, Free vibration and lateral buckling of a cantilever slender beam with an edge crack: experimental and numerical studies, *Journal of Sound and Vibration,* Vol. 326, No. 1-2, pp. 235-250, 2009.